A&A 391, 13–20 (2002)
DOI: 10.1051/0004-6361:20020792

Astronomy & Astrophysics

Constraints on $(\Omega_m, \Omega_\Lambda)$ using distributions of inclination angles for high redshift filaments

M. Weidinger[1], P. Møller[2], J. P. U. Fynbo[2], B. Thomsen[1], and M. P. Egholm[1]

[1] University of Aarhus, Ny Munkegade, 8000 Århus C, Denmark
[2] European Southern Observatory, Karl-Schwarzschild-Straße 2, 85748, Garching by München, Germany

Received 20 February 2002 / Accepted 23 May 2002

Abstract. In this paper we present a scale free method to determine the cosmological parameters $(\Omega_m, \Omega_\Lambda)$. The method is based on the requirement of isotropy of the distribution of orientations of cosmological filaments. The current structure formation paradigm predicts that the first structures to form are voids and filaments, causing a web-like structure of the matter distribution at high redshifts. Recent observational evidence suggests that the threads, or filaments, of the cosmic web most easily are mapped in Lyα emission. We describe how such a 3D map can be used to constrain the cosmological parameters in a way which, contrary to most other cosmological tests, does not require the use of a standard rod or a standard candle. We perform detailed simulations in order to define the optimal survey parameters for the definition of an observing programme aimed to address this test, and to investigate how statistical and observational errors will influence the results. We conclude that observations should target filaments of comoving size 15−50 Mpc in the redshift range 2−4, and that each filament must be defined by at least four Lyα emitters. Detection of 20 filaments will be sufficient to obtain a result, while 50 filaments will make it possible to place significant new constraints on the values of Ω_m and Ω_Λ permitted by the current supernova observations. In a future paper we study how robust these conclusions are to systematic velocities in the survey box.

Key words. cosmology: theory – cosmological parameters

1. Introduction

Recent studies have successfully narrowed down the permitted parameter space for the cosmological parameters Ω_m and Ω_Λ. Confidence intervals defined by observations of distant supernovae (Riess et al. 1998; Perlmutter et al. 1999) and those resulting from the high-resolution observations of the cosmic microwave background radiation (CMB) (Jaffe et al. 2000) meet almost orthogonally, and as a result they combine to bracket a domain of high probability. There remains, however, the question of possible systematic effects which may produce significant errors (e.g. Simonsen & Hannestad 1999; Rowan-Robinson 2002). It is therefore important that new and independent methods to determine Ω_m and Ω_Λ should be sought and exploited.

The classic cosmological tests (Sandage 1961) involve the use of either standard rods or standard candles. The supernovae projects for example, are based on the use of standard candles, while recent proposals to use the distribution of Lyman Break Galaxies and arrangements of Lyα-forest systems (Roukema 2001; McDonald & Miralda-Escudé 1999 respectively) involve the use of standard rods. The potential worry with all such methods is that the hypothetical standard rods or candles may in reality not be good standards because of evolutionary effects, or simply because the evolution of structure may be a fractal process without any preferred scale.

The simplest and cleanest cosmological tests one might imagine would be a purely geometric test not involving measurements of standard rods. The first such method was proposed by Alcock & Paczyński (1979), who considered an idealized set of objects distributed spherically symmetric and on average following the Hubble flow. The idea is beautiful in its simplicity, but the requirement of spherical symmetry of the distribution (requiring a length scale to be the same in all directions) is in reality an indirect use of a standard rod, even if at a single point in redshift space. The hypothetical spherical distribution might as well be ellipsoidal, which would then invalidate the result. The question is if it is at all possible to devise a geometrical test not requiring any length scale at all.

Numerical simulations of early structure formation based on the Cold Dark Matter scenario (Klypin & Shandarin 1983; White et al. 1987; Rauch et al. 1997) show that high redshift star-forming regions tend to align themselves in long filaments with a higher-than-average matter density. This has recently

Send offprint requests to: M. Weidinger,
e-mail: michaelw@ifa.au.dk

been confirmed observationally by Møller & Fynbo (2001), who also pointed out that such structures offered three independent cosmological tests, all of which were purely geometric, and none of which required the early structure formation to have a preferred length scale. The only requirement is that of global isotropy. The first of those three tests concerns the distribution of filament inclination angles which, in an isotropic universe, must be random. In this paper we present a detailed analysis, based on Monte Carlo simulations, of this first filament test.

The paper is organized as follows: In Sect. 2 we introduce the method, in Sect. 3 we describe the details of the simulations and interpret the results in a cosmological context to see which constraints we may put on the cosmological parameters, in Sect. 4 we address some additional sources of statistical and observational errors, and use the results to define the optimal survey parameters for an observing programme, and finally in Sect. 5 we summarize the results and conclusions. We have included a short appendix, which briefly introduces the notation and the necessary cosmological relations.

2. $F(\Omega_m, \Omega_\Lambda, z)$: The line of sight scale factor

The cosmological principle tells us that any class of elongated objects or structures will, at all redshifts, display a random distribution of orientations of their major axes. Elongated structures that are so large that they are everywhere anchored in the local Hubble flow are usually referred to as "filaments" and "walls", and for such objects the cosmological redshift will vary along the structures and thereby reveal their orientations in 3D redshift space. The basis of the cosmological test described here is to determine the sets of $(\Omega_m, \Omega_\Lambda)$ which, at any given redshift, will make the observed distribution of orientations anchored in the Hubble flow conform to this requirement of isotropy.

As a simple example let us first consider an area on the sky in the form of a square with sides of angular size ϕ. At any given redshift z this will correspond to a square in the plane of the sky with sides of proper size

$$W_{\rm true} = \frac{\phi}{H_0} f_W(\Omega_m, \Omega_\Lambda, z) \tag{1}$$

where prescriptions for calculation of f_W (as well as of f_L below) are provided in Appendix A. If we further consider a redshift interval δz centred on z, we have defined a box of proper length

$$L_{\rm true} = \frac{\delta z}{H_0} f_L(\Omega_m, \Omega_\Lambda, z). \tag{2}$$

Let the box be filled with a large number of filaments, and let their distribution of orientations be isotropic. If one were to either stretch or squeeze the box along the line of sight (along the redshift direction), the angular distribution of the filaments would (because they are anchored in the Hubble-flow) no longer remain isotropic.

For illustration purposes it is useful to think of a box inside which an isotropic network of rubber bands has been mounted between opposing walls. If we stretch the box along one direction the angles between the rubber bands and the stretching direction will all decrease. If, instead, we were to stretch the box by that same factor in *all* directions, the angles would remain unchanged. Hence, in considering observationally only the distribution of *angles*, one is not gaining any information about true sizes. By the same token, since the true size of an object falls out of the equations, the test that we describe here does not require the existence of a "standard rod" at any redshift.

Because the actual length and width of the box is irrelevant for our test, the only numerical value of interest is the "change of scale" between the two directions (along the line of sight and perpendicular to the line of sight). What we are interested in is therefore the ratio between the length and the width

$$\frac{L}{W} = \frac{\delta z}{\phi} \frac{f_L(\Omega_m, \Omega_\Lambda, z)}{f_W(\Omega_m, \Omega_\Lambda, z)} \tag{3}$$

and how the *apparent* value of that ratio relates to its *true* value

$$F(\Omega_m, \Omega_\Lambda, z) = \frac{(L/W)_{\rm app}}{(L/W)_{\rm true}}. \tag{4}$$

Note that H_0, ϕ, and δz have cancelled out of the ratio $F(\Omega_m, \Omega_\Lambda, z)$. In what follows we shall refer to this ratio as the *"line of sight scale factor"*.

Returning briefly to the example above, for a given triple of observables $(\phi, z, \delta z)$ and an assumed cosmology $(\Omega_m, \Omega_\Lambda)$, the box is fully defined. If one now assumes a different cosmology, the inferred size of the box will change. For most choices of cosmology, the change in length and width of the box will be different (hence the value of F will change), but it is always possible to find sets of $(\Omega_m, \Omega_\Lambda)$ with the combined effect of changing both length and width by the same factor, thereby keeping F constant. In Fig. 1 we show a set of such "isoscale curves" (curves of constant F) for a redshift of 3. Our test can now be formulated simply: "Determine the sets of $(\Omega_m, \Omega_\Lambda)$ for which $F = 1$". The remainder of this paper is concerned with the formulation of how this is done in practice. In addition we use Monte Carlo simulated data to determine what level of accuracy may be reached with current telescopes and instrumentation.

3. Limits on F from Monte Carlo simulations

Consider a large number of idealized, randomly aligned, linear and thin filaments. Let the inclination angle θ of a filament be the angle between the filament major axis and our line of sight to the filament. A filament pointing towards us will hence have inclination angle zero, and the cumulative distribution of isotropically distributed inclination angles can be shown to be

$$P(x) = 1 - \frac{1}{\sqrt{1 + \tan^2 x}}, \tag{5}$$

where $x \in [0, \pi/2]$ and $P(x)$ is the probability of observing an inclination angle $\theta < x$. If we now use a wrong set of values $(\Omega_m, \Omega_\Lambda)$, then the *apparent* distributionis no longer isotropic

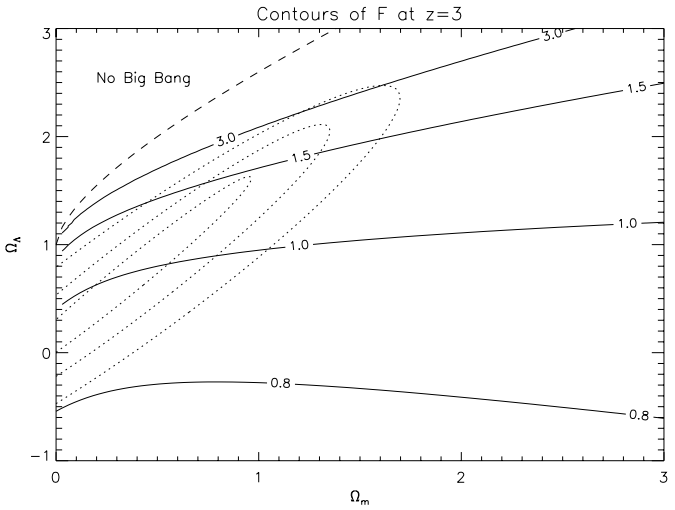

Fig. 1. Solid: contours of constant value of the dimensionless line of sight scale factor F (here for $z = 3$ and normalized to $F = 1$ for $\Omega_m = 0.3$, $\Omega_\Lambda = 0.7$). Dotted: 68.3%, 95.4% and 99.7% confidence regions obtained by supernovae observations (Riess et al. 1998).

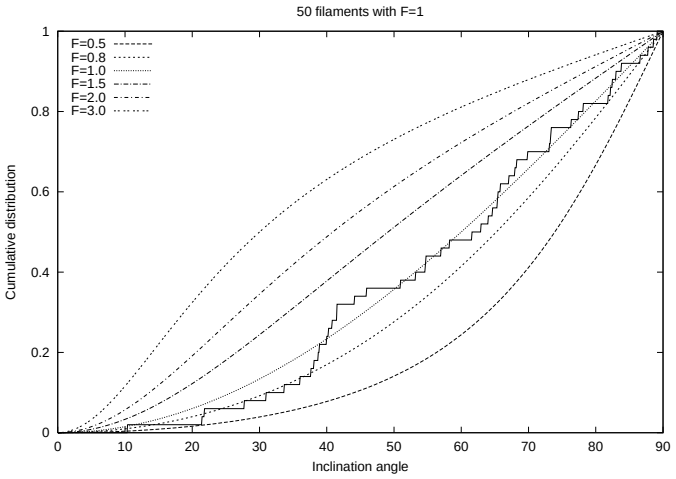

Fig. 2. Cumulative distribution of Monte Carlo simulation of 50 filaments, compared to expected distributions for a range of values of the line of sight scale factor F.

and the accumulated distribution of inclination angles is instead given by the general expression

$$P(x, F) = 1 - \frac{1}{\sqrt{1 + F^2 \tan^2 x}}, \quad (6)$$

where F is the line of sight scale factor (Eq. (4)).

Given a set of observed inclination angles, a K–S test (Press et al. 1989) against $P(x, F)$, can be used to determine the value of F which best fits the observed distribution. At present there is no data set available large enough to place useful constraints on the cosmological parameters. Instead we have created Monte Carlo data in order to determine how large a data set we shall need to be able to set interesting limits. The K–S test is only valid for fairly large samples, so in addition we have tested a number of alternative estimators all based on the comparison of cumulative distributions. The classic K–S test only seeks to minimize the largest difference between the two cumulative distributions. For small samples we found that the scatter of the fit was smaller when we minimized the sum of the square of the difference at *each* entry in the sample (Eq. (7)), while for large samples the two methods gave identical scatter.

The samples of simulated filaments were computed by randomly selecting N inclination angles, θ_i, such that the values of $\cos\theta_i$ formed a uniform distribution between 0 and 1. For each such sample we used the extended K–S test described above and determined the best fitting value of F by minimization of $D(F)$:

$$D(F) = \sum_{i=1}^{N} d_i^2, \quad (7)$$

where $d_i = \max\left(\left|\frac{i}{N} - P(\theta_i, F)\right|, \left|\frac{i-1}{N} - P(\theta_i, F)\right|\right)$, and P is defined in Eq. (6). As an illustration we show in Fig. 2 the cumulative distribution of a realization of 50 filaments (histogram) and the predicted distribution for a range of values of F (lines) based on Eq. (6).

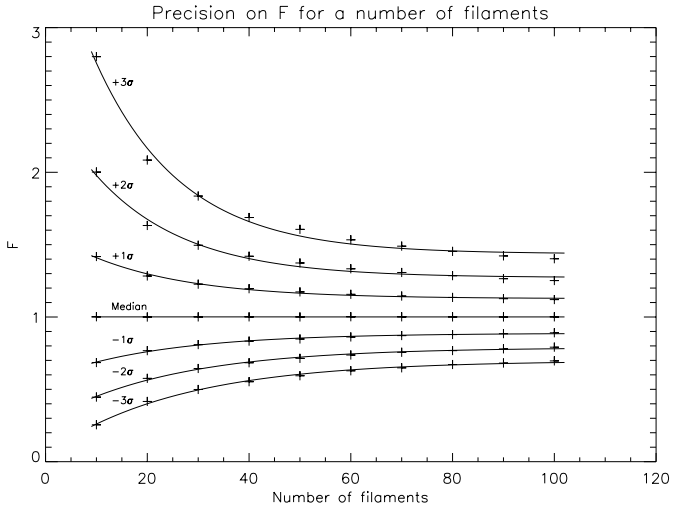

Fig. 3. Plot of the uncertainty with which we can determine the stretching factor F as a function of how many filaments are in our sample. This is the result of 2×10^4 simulations for each number of filaments. The upper and lower 1, 2 and 3σ uncertainties are fitted with exponentials. The result is given in Table 1.

It is now interesting to ask how many filaments one would need to observe, to be able to place cosmologically interesting limits on the observed value of F. To address this question we repeated the simulations for the range 10 to 100 filaments in steps of 10, and in each case running 2×10^4 simulations. The results are shown in Fig. 3. The one-sided 1, 2 and 3σ curves were found as the 15.9%, 2.28% and 0.13% quantiles. The 1, 2, and 3σ curves are fitted well by the exponential functions given in Table 1. The median is consistent with a straight line with intercept 1.00 and slope 0.000.

As illustrated in Fig. 1, each value of F represents, at a given redshift, a curve in the (Ω_m, Ω_Λ) diagram. Using the cosmological relations given in Appendix A, we can therefore transform our limits on F (Fig. 3) into a set of curves confining the permitted cosmologies (Fig. 4). Part of the parameter

Table 1. The $n\sigma$ errors fitted with $F(N) = ae^{bN} + c$.

$n\sigma$	a	b	c
$+3\sigma$	2.67	−0.0650	1.45
$+2\sigma$	1.25	−0.0560	1.27
$+1\sigma$	0.482	−0.0507	1.13
-1σ	−0.313	−0.0451	0.887
-2σ	−0.498	−0.0396	0.791
-3σ	−0.671	−0.0417	0.694

space in Fig. 4 represents "bouncing" universes that do not expand monotonically from a Big Bang. This corresponds to the region in the figure where $\Omega_\Lambda > 4\Omega_m\, x^3$, in which

$$x = \begin{cases} \cosh\left[\frac{1}{3}\cosh^{-1}(\Omega_m^{-1} - 1)\right] & \text{when } 0 < \Omega_m \le \frac{1}{2} \\ \cos\left[\frac{1}{3}\cos^{-1}(\Omega_m^{-1} - 1)\right] & \text{when } \frac{1}{2} \le \Omega_m \end{cases} \quad (8)$$

(Felten & Isaacman 1986). In this region of the figure, the expression $(1+z)^2\,(\Omega_m z + 1) - \Omega_\Lambda z\,(z+2)$ under the square-root in the equation for $\frac{dr}{dz}$ (see Appendix A) becomes negative for some z (the sign of the expression shifts when the universe changes from expansion to contraction and vice versa). We do not calculate F in this region.

The contours of F in Fig. 4 are calculated for $z = 3$, for 20 and 50 filaments, and are normalized to $F = 1$ for an $\Omega_m = 0.3$, $\Omega_\Lambda = 0.7$ universe. For easy comparison, the confidence regions obtained by supernovae observations (Riess et al. 1998) are also plotted. Two interesting points are immediately obvious from Fig. 4. First it is seen that the isoscale curves are mostly horizontal, and that they place tight upper limits on Ω_Λ almost independently of Ω_m. This is contrary to the corresponding confidence limits from the supernovae observations which span diagonal regions in the diagram. Secondly it is seen that already with a sample of 20 filaments one would set upper limits on the value of Ω_Λ intersecting those currently set by the high z SN studies. Such a limited study would therefore not only provide a new and independent way to determine Ω_Λ, it would already serve to further constrain the parameter space allowed by the SN studies. For 50 filaments the intersections would be such that they would reduce the area of the 1σ upper confidence limit set by the SN studies by 30%.

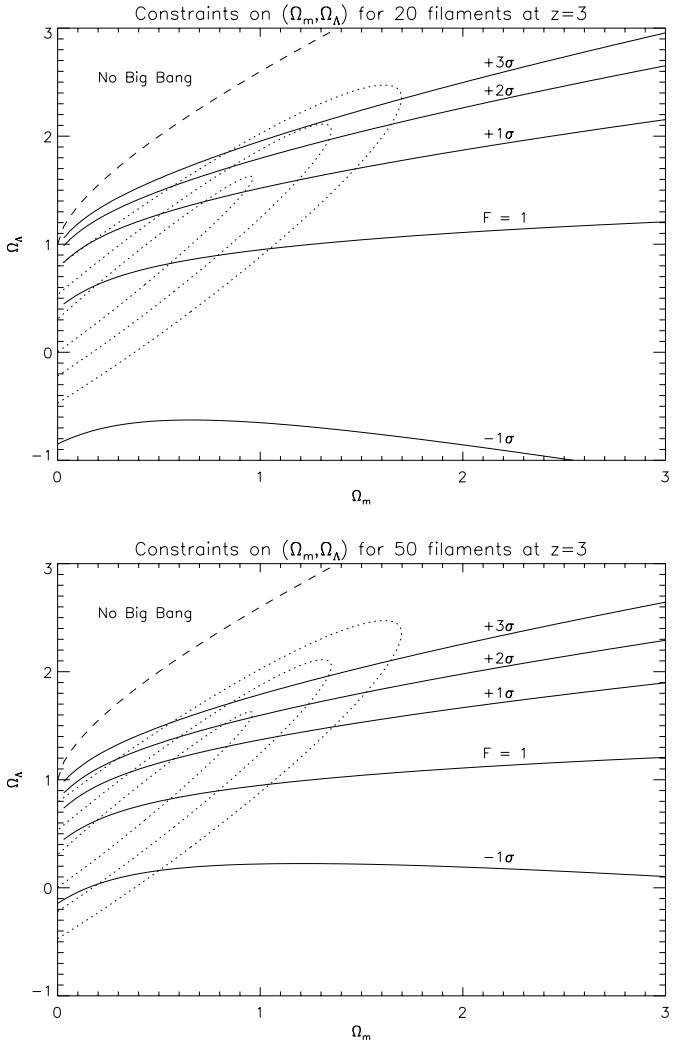

Fig. 4. Solid: confidence limits on F for observations of 20 (upper plot) and 50 (lower plot) filaments at $z = 3$, normalized to $\Omega_m = 0.3$, $\Omega_\Lambda = 0.7$. Dotted: the 68.3% (smallest), 95.4% and 99.7% (largest) confidence regions obtained by supernovae observations.

4. Observational implementation of the test

4.1. The optimal redshift range

For the planning of an observing campaign to carry out the proposed test, it is useful first to consider at which redshifts the test is most sensitive to realistic values of Ω_Λ, and how one may best identify filaments at those redshifts. In Fig. 5 we plot F as a function of redshift for several different cosmological models, also here normalized so that $F = 1$ corresponds to the $\Omega_m = 0.3$, $\Omega_\Lambda = 0.7$ model. The dotted and dashed curves below the $F = 1$ line correspond to $\Omega_\Lambda = 0$ models with $\Omega_m = 1$ and $\Omega_m = 0.3$ respectively. The dot-dashed curves above the $F = 1$ line correspond to models with $\Omega_\Lambda > 0.7$ (see caption for details). All curves converge at $F = 1$ in the limit of zero redshift. It is seen that for all models with $\Omega_\Lambda < 1$, F is almost independent of redshift in the redshift range $z \approx 1.5$–4, while F grows monotonically with redshift for models with $\Omega_\Lambda > 1$. Hence, in order to test against any cosmology with $\Omega_\Lambda < 1$ one should select the redshift in the range 1.5–4 where filaments are most easily detected.

4.2. Filament identification and sparse sampling errors

Lyα narrow band imaging has proven an efficient technique for identification of high redshift filaments (Møller & Warren 1998; Møller & Fynbo 2001). Confirming spectroscopy then maps out filaments as strings of separate star forming regions, each glowing in Lyα. In what follows we shall refer to those Lyα emitting regions using the shorter name "LEGOs" (Lyα Emitting Galaxy-building Objects). Since each filament in this way is mapped by a finite number of objects, the accuracy with

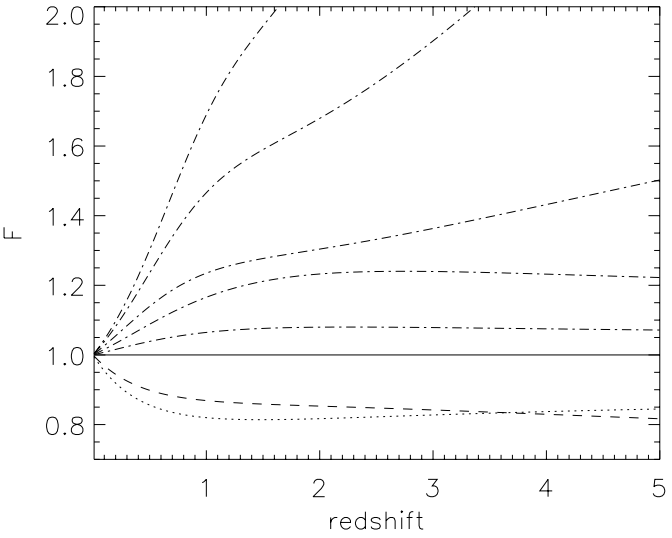

Fig. 5. We plot F as a function of redshift for a range of cosmological models. $F = 1$ corresponds to the $\Omega_m = 0.3$, $\Omega_\Lambda = 0.7$ model. The dotted and dashed curves below the $F = 1$ line correspond to $\Omega_\Lambda = 0$ models with $\Omega_m = 1$ and $\Omega_m = 0.3$ respectively. The dot-dashed curves above the $F = 1$ line correspond to models with (Ω_m,Ω_Λ) = (0.2,0.8), (0.1,0.9), (0.3,1.2), (0.3,1.4), (0.3,1.5).

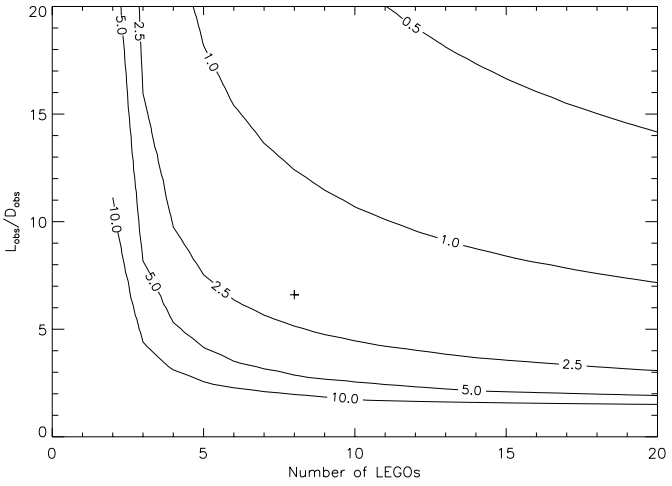

Fig. 6. Contours of constant sparse sampling error on filament orientation as a function of the number of LEGOs defining the filament and the length-to-diameter ratio L_{obs}/D_{obs}. The contours are $\sigma_{sp} = 0.5°$, 1°, 2.5°, 5° and 10°, and the cross marks the filament detected by Møller & Fynbo (2001). The contours are based on 10^6 runs at each point.

which one may determine its inclination angle will be a function of the number of LEGOs defining it.

As for the optimal redshift range and number of filaments, it is useful to consider what may be the minimum number of LEGOs needed per filament for an adequate determination of its inclination angle. To address this question we ran a series of simulations in which we randomly placed N LEGOs inside filaments defined as cylinders of length L and diameter D. We then determined the "observed" orientation vector of each filament, (defined as the best fitting straight line through the N points), and the "observed" length-to-diameter ratio, L_{obs}/D_{obs}[1]. The observed set of orientation vectors define a solid angle centred on the true orientation vector, from which the sparse sampling error (σ_{sp}) may be determined directly as the RMS of the 2D distribution of the observed set of intersections between the orientation vectors and the surface of the unit sphere. In Fig. 6 we show contours of constant σ_{sp} as a function of N and the L_{obs}/D_{obs} ratio. As one would expect σ_{sp} is small for long/thin filaments but larger for short/wide filaments. It is also seen that for filaments defined by fewer than four LEGOs σ_{sp} grows rapidly. Møller & Fynbo (2001) reported the detection of a filament at $z = 3.04$ defined by eight LEGOs. Assuming (Ω_m,Ω_Λ) = (0.3, 0.7) and using the procedure outlined above, we find $L_{obs} = 20.2$ Mpc and $D_{obs} = 3.2$ Mpc (comoving) for the $z = 3.04$ filament, and an inclination angle of 25.5°. Its position is marked in Fig. 6 and it is seen that the sparse sampling error on its orientation is ≈1.9°.

[1] The length of the cylinder is found as $L_{obs} \equiv \sqrt{12}$ RMS(z), and the diameter $D_{obs} \equiv \sqrt{8}$ RMS(r), where z is the position of a point projected onto the axis of symmetry, and r is the distance of a point to the axis of symmetry.

Table 2. Errors (1σ) on determination of the line of sight scale factor F (Fig. 3) including sparse sampling of individual filaments. The results are based on 2×10^5 runs.

	Filaments		
σ_{sp}	20	50	80
0.0°	0.259	0.162	0.128
5.0°	0.265	0.166	0.131
10.0°	0.283	0.179	0.140

In order to propagate the sparse sampling errors shown in Fig. 6 to errors on the determination of the line of sight scale factor F, we repeated the Monte Carlo simulations of Sect. 3, now including random errors on filament orientations as described above. The goal was to determine how large intrinsic errors on the filament orientations we could tolerate before the error analysis summarised in Fig. 3 would be seriously compromised. The Monte Carlo simulations were repeated for 20, 50, and 80 filaments, and for σ_{sp} in the range 0° to 10°. The results are summarised in Table 2 where we list errors on F from Fig. 3, and from the full analysis including sparse sampling errors. It is seen that even for σ_{sp} as large as 10° the additional errors are insignificant. From Fig. 6 we see that $\sigma_{sp} < 10°$ always is achieved for filaments with $L_{obs}/D_{obs} > 3$ defined by four LEGOs or more.

In conclusion of this section, a first rough determination of (Ω_m, Ω_Λ) can be obtained with the discovery of 20 filaments each defined by four LEGOs, or 80 LEGOs in all. With 50 filaments, or 200 LEGOs total, the errors are such that they will place significant new constraints on the values of Ω_m and Ω_Λ permitted by the current supernova observations.

4.3. Optimal survey box size

Up till this point we have discussed the error budget caused by purely statistical errors only; errors arising from a finite filament sample and from the finite number of objects defining each filament. Those errors are scale invariant and place no constraints on the size of the survey box. For observational reasons there is an upper bound to the size of the volume we are able to survey to the necessary flux limit. On the other hand we can only identify filaments of sizes smaller than the chosen survey box, and if that box is too small then measurement errors and errors caused by motion relative to the Hubble flow could become dominant. One may consider two types of motion relative to the Hubble flow; "random motion" and "bulk flow" (streaming).

4.3.1. Random velocities and measurement errors

Random velocities and measurement errors are most efficiently treated together because errors on the redshift are independent from random radial motion and therefore adds in quadrature. Let us consider the filament reported by Møller & Fynbo (2001). In this case the error on the redshift determination of the Lyα lines was 50 km s^{-1} (Fynbo et al. 2001). At $z \approx 0$ the typical peculiar velocity is 200 km s^{-1} (Branchini et al. 2001). This includes both random motion and systematic flows towards large dark matter haloes, and can therefore be considered a firm upper limit to the random peculiar velocities at high redshifts. Only the radial component (100 km s^{-1}) of the random velocity vector is observed, and in combination with the typical redshift measurement error we have a 112 km s^{-1} radial error. This corresponds to d$z = 0.0015$ at $z = 3$, or to 9% of the length of the filament (390 kpc in an $\Omega_m = 0.3$, $\Omega_\Lambda = 0.7$, $h = 0.65$ universe). To understand the effects on a survey for filaments, let us consider the two limiting cases of filaments with $\theta = 0°$ and $\theta = 90°$. For $\theta = 0°$ the filament is aligned along our line of sight, and the additional scatter (RMS = 9% of total length) along the filament will simply make it look at bit longer than it is in reality. Hence the L_{obs}/D_{obs} ratio will be overestimated by a miniscule amount, and σ_{sp} will be similarly underestimated. Since σ_{sp} is already irrelevantly small, this will have no consequences for the cosmological test. Considering now the case $\theta = 90°$ (a filament perpendicular to the line of sight) we see that in this case the measured diameter of the filament (800 kpc) will be increased (along the line of sight) by the added scatter, resulting in an added error on the determination of the inclination angle. The added error can be found from Fig. 6 via calculation of the predicted L_{obs}/D_{obs} ratio. The filament considered here would (had it been found to have $\theta = 90°$) have had a diameter increase of 70% along the line of sight. Hence L_{obs}/D_{obs} would have changed from 6.6 to 3.9, and the corresponding sparse sampling error from 1.9° to 3.4°. From Table 2 we see that this 70% increase has no effect, but with another factor of two those errors would become dominating.

Errors perpendicular to the line of sight are typically a fraction of an arcsec, or about two orders of magnitude less than those along the line of sight. Those can be completely ignored. A side-effect of this "orders of magnitude difference" is that thin filaments with *small* inclination angles will appear observationally as thin filaments (strings), while thin filaments with *large* inclination angles will appear to have cross-sections which are elongated along the line of sight (ribbons). Observational determination of the magnitude of this "ribbon effect" will make it possible to determine the *actual* RMS of the non-Hubble flow velocities at $z = 3$ (the 200 km s^{-1} we used in this example is, as mentioned above, to be regarded as an upper limit).

The 20 Mpc filament considered above remains fully defined when we include expected random errors. However, we see from Fig. 6 that a similar filament defined by only 4 LEGOs would move close to the curve marking the 10° sparse sampling error. Therefore, because of the expected magnitude of the errors caused by random motion, it will in general not be possible to determine inclination angles with sufficient precision for filaments significantly shorter than 15 Mpc. Filaments significantly larger than 50 Mpc are still prohibitively difficult to identify for observational reasons, so at present an optimal search for filaments at $z = 3$ must target filaments of comoving length 15−50 Mpc. The optimal survey box has sides of length 50−60 Mpc.

4.3.2. Systematic peculiar velocities

The final point we shall consider is the effect of bulk flow in the survey box. First we address the scale dependence. Any bulk motion on the same scale as the filaments themselves, or larger, will simply result in a translation of an entire filament and hence have no influence on the distribution of angles. Bulk motion on scales much smaller than the filaments will appear as random motion (treated in the previous section). Therefore, only bulk motion in the regime between those two limits (several, but not all, LEGOs in a single filament) is relevant.

It is at present not easy to predict precisely what sort of bulk motion will be present on this scale. In the local universe we see large scale streaming towards massive dark matter halos, but since this is the result of acceleration over a Hubble time one would expect similar streaming at higher redshifts to have smaller amplitude. In simulations of the early universe two types of flows are seen. First it is often seen that protogalaxies in the filaments stream along the filaments towards the nodes, second it is seen that nodes are attracted to each other. The "streaming towards nodes" will have the effect of making the filaments appear longer than they are (stretching), the movement of nodes towards each other will have the opposite effect (squeezing). To first order one might expect that the two effects cancel each other, but it is equally possible that one of the two dominates. If the latter is the case, it will cause a systematic error on the determination of F.

In the previous sections we have outlined how to determine F from a set of data. Those data could be observational, but they could equally well be taken from a simulation. The only way to address the possible effect of intermediary scale bulk motion is to apply our method to sets of filaments in simulated volumes. We shall return to the results of this work in a separate paper.

5. Summary and conclusions

A significant number of 8−10 meter class telescopes became operational during the past decade, thereby moving several cosmological tests from the domain of speculation into the domain of observation. The currently most successful test relies heavily upon the assumption that supernovae of type Ia are standard candles. Other proposed tests, based on e.g. distances between Lyman Break galaxies, seek to exploit an expected standard rod.

In this paper we have presented a detailed discussion of a test which relies on neither standard candles nor standard rods. The test makes use of only the requirement of isotropy, and of the prediction from numerical simulations of the high redshift universe that it has a filamentary structure. Direct observational evidence that such filaments may indeed be found was presented by Møller & Fynbo (2001) who also proposed three cosmological tests based on the existence of such filaments. Here we have in detail investigated and described the implementation of the first of these tests. We have used Monte Carlo simulations to determine the accuracy with which one may obtain values of Ω_m and Ω_Λ, and we have described how additional statistical errors and observational effects will affect the results. Guided by the detailed Monte Carlo simulations, and taking into account the capabilities of current instrumentation, we have considered what would be the optimal survey parameters for an observing campaign aimed at an implementation of this test.

We find that the constraints this test can set are mostly on Ω_Λ, or in other words the limiting curves in the usual (Ω_m, Ω_Λ) diagram are mostly horizontal. This means that they intersect the probability curves from the $z < 1$ SN Ia projects. Already with a sample of only 20 filaments the SN Ia results will be intersected, but with a sample of 50 filaments the area of allowed values in the (Ω_m, Ω_Λ) diagram will be significantly reduced. The optimal redshift range for the test is found to be $z = 1.5$−4. In the range $z = 2$−4 filaments can conveniently be detected using deep searches for faint Lyα emitters (LEGOs). Each filament to be used in this test must have an observed length-to-diameter ratio of no less than 3, and must be defined by no less than four objects.

We have considered the effect of random and systematic non-Hubble flow velocities. There are no observational determinations of peculiar velocities at high redshifts yet, so their impact is discussed in qualitative terms mostly. A detailed analysis of those effects, which are important as they set the minimum scale size of structures which will be useful for the test, will be presented in a future paper. However, using the local RMS value for peculiar velocities (which we consider a realistic upper limit), we find that the optimal survey box is a cube with sides of length 50−60 comoving Mpc.

Three surveys are currently underway which should produce data useful for this test: i) the Large Area Lyman Alpha (LALA) survey (Rhoads et al. 2000) that targets Lyα emitters at redshift 4.5 and 5.7, ii) a survey conducted with the SUBARU telescope which has resulted in a large sample of candidate Lyα emitters at $z = 4.86$ (Ouchi et al. 2002), and iii) in the opposite end of the optimal redshift window there is a survey on the Nordic Optical Telescope (NOT) to map out a slice of the $z = 2$ universe in Lyα emission (Møller et al. in prep.). The NOT survey started in 2001 and takes advantage of the excellent UV capabilities of the NOT instrumentation which was demonstrated in similar observations of fields containing $z = 2$ host galaxies of Gamma Ray Bursters (Fynbo et al. 2002). Currently there are no large area Lyα surveys targeting $z = 3$, and there are no large area Lyα surveys conducted on the ESO VLT. Smaller targeted programmes aimed at $z = 3$ fields have been successfully conducted on the VLT (Fynbo et al. in prep.), confirming that the necessary volume density of Lyα emitters will indeed be found.

Acknowledgements. We are grateful to H.-J. Gerber for interesting discussions, and for helpful comments on an earlier version of this manuscript. MPE and MW acknowledge support from the ESO Directors Discretionary Fund.

Appendix A: Cosmology with $\Lambda \neq 0$

We follow the treatment given in Longair (1998), which uses the metric in the form:

$$ds^2 = c^2dt^2 - R^2(t)[dr^2 + \mathcal{R}^2 \sin(r/\mathcal{R})^2(d\theta^2 + \sin(\theta)^2 d\phi^2)], \quad (A.1)$$

where $\mathcal{R}$ is the radius of curvature of the universe, and R is the scale factor normalized to 1 at the present epoch. The radial coordinate r is the metric distance at time t, and it can be found as a function of z by integrating the differential equation

$$\frac{dr}{dz} = \frac{c}{H_0}\left((1+z)^2(\Omega_m z + 1) - \Omega_\Lambda z(z+2)\right)^{-1/2}, \quad (A.2)$$

where Ω_m and Ω_Λ are given by the present mean density ρ_0 and the cosmological constant Λ, respectively:

$$\Omega_m = \frac{8\pi G\rho_0 c^2}{3H_0^2}, \quad \Omega_\Lambda = \frac{\Lambda c^2}{3H_0^2}. \quad (A.3)$$

The radius of curvature $\mathcal{R}$ can be determined from the relation

$$\frac{1}{\mathcal{R}^2} = \frac{\Omega_m + \Omega_\Lambda - 1}{c^2/H_0^2}. \quad (A.4)$$

Longair defines the distance measure

$$D = \begin{cases} \mathcal{R}\sin(r/\mathcal{R}) & \text{if } 1/\mathcal{R}^2 > 0 \\ r & \text{if } 1/\mathcal{R}^2 = 0 \\ \mathcal{R}\sinh(r/\mathcal{R}) & \text{if } 1/\mathcal{R}^2 < 0 \end{cases} \quad (A.5)$$

from which the angular diameter distance D_A can be derived as $D_A = D/(1+z)$. The proper radial distance is determined from the differential $\left(\frac{dr}{dz}\right)_{prop} = \frac{dr}{dz}/(1+z)$.

We can now finally derive the two functions f_L and f_W introduced in Sect. 2. As $W_{true} = \phi D_A$ the function f_W is simply given by $H_0 D_A$. Similarly, the proper length L_{true} of a box defined by two redshifts z_{min} and z_{max} ($\delta z = z_{max} - z_{min} \ll (z_{max} + z_{min})/2$) is given by $\left(\frac{dr}{dz}\right)_{prop}\delta z$, hence $f_L = H_0\left(\frac{dr}{dz}\right)_{prop}$.

References

Alcock, C., & Paczyński, B. 1979, Nature, 281, 358

Branchini, E., Freudling, W., Da Costa, L. N., et al. 2001, MNRAS, 326, 1191

Felten, J. E., & Isaacman, R. 1986, Rev. Mod. Phys., 58, 689

Fynbo, J. P. U., Møller, P., & Thomsen, B. 2001, A&A, 374, 443

Fynbo, J. P. U., Møller, P., Thomsen, B., et al. 2002, A&A, 388, 425

Jaffe, A. H., Ade, P. A. R., Balbi, A., et al. 2000, Phys. Rev. Lett., 86, 3475

Klypin, A. A., & Shandarin, S. F. 1983, MNRAS, 204, 891

Longair, M. S. 1998, in Galaxy Formation, A&A Library, ed. I. Appenzeller, G. Börner, M. Harwit, et al. (Springer Verlag), chapter 7

McDonald, P., & Miralda-Escudé, J. 1999, ApJ, 518, 24

Møller, P., & Warren, S. J. 1998, MNRAS, 299, 661

Møller, P., & Fynbo, J. P. U. 2001, A&A, 372, L57

Ouchi, M., Shimasaku, K., Furusawa, H., et al. 2002, ApJ, submitted [astro-ph/0202204]

Perlmutter, S., Aldering, G., Goldhaber, G., et al. 1999, ApJ, 517, 565

Press, W. H., Flannery, B. P., Teukolsky, S. A., & Vetterling, W. T. 1989, Numerical Recipes (Cambridge University Press)

Rauch, M., Haehnelt, M. G., & Steinmetz, M. 1997, ApJ, 481, 601

Rhoads, J. E., Malhotra, S., Dey, A., et al. 2000, ApJ, 545, L85

Riess, A. G., Filippenko, A. V., Challis, P., et al. 1998, ApJ, 116, 1009

Roukema, B. F. 2001, A&A, 369, 729

Rowan-Robinson, M. 2002, MNRAS, 332, 352

Sandage, A. 1961, ApJ, 133, 355

Simonsen, J. T., & Hannestad, S. 1999, A&A, 351, 1

White, S. D. M., Frenk, C. S., Davis, M., & Efstathiou, G. 1987, ApJ, 313, 505